ELSEVIER

Biochimica et Biophysica Acta 1188 (1994) 325–334

BBA Biochimica et Biophysica Acta

Investigation of the ammonium chloride and ammonium acetate inhibition of oxygen evolution by Photosystem II

Dugald J. MacLachlan [a], Jonathan H.A. Nugent [a,*], Joseph T. Warden [b], Michael C.W. Evans [a]

[a] *Department of Biology, Darwin Building, University College London, Gower Street, London WC1E 6BT, UK*
[b] *Department of Chemistry, Rensselaer Polytechnic Institute, Troy, NY 12180–3590, USA*

Received 17 May 1994; revised 30 August 1994

Abstract

Using EPR and EXAFS spectroscopies we show that high concentrations of ammonium cations at alkaline pH are required for (1) inhibition of oxygen evolution: (2) an alteration of the EPR properties of the oxygen evolving complex: (3) the ability to detect $Y_Z^{\cdot}$; and (4) the slow reduction of the Mn complex leading to the appearance of EPR detectable Mn^{2+}. The inhibition of S state cycling, slowing of $Y_Z^{\cdot}$ reduction, appearance of Mn^{2+} and the yield of a Hpp < 10 mT S_3 type EPR signal are decreased by calcium addition. This indicates that these effects were probably associated with calcium depletion arising from the high concentration of ammonium cation. The ammonia-induced changes to the S_2 multiline EPR signal are not affected by calcium addition. The appearance of Mn^{2+} is shown to be reversible on illumination, suggesting that the Mn reduced from the native state is located at or near the native site. Simulations of the interaction which gives rise to the S_3 EPR signal are also presented and discussed. These indicate that lineshape differences occur through small changes in the exchange component of the interaction between the manganese complex and organic radical, probably through minor structural changes between the variously treated samples.

Keywords: Oxygen evolving complex; Manganese; EXAFS; EPR; Calcium

1. Introduction

Photosystem II (PS II) is a membrane–protein complex which reduces plastoquinone to plastoquinol using electrons supplied by photosynthetic water oxidation (see Refs. [1–4] for reviews). Within PS II the main electron transfer pathway is located in the reaction centre polypeptides D1 and D2. Charge separation and stabilisation is initiated by excitation of the reaction centre pigment, P680, which then oxidises the Mn-containing oxygen-evolving complex (OEC) via tyrosine Y_Z, Tyr 161 of D1 [5,6]. Four turnovers of the OEC are required for water oxidation resulting in five states denoted S_i, $i = 0,\ldots,4$. Efficient function of the water oxidising enzyme also requires the inorganic cofactors calcium and chloride [1–4,7,8]. A second redox active tyrosine residue, Y_D, has been identified as Tyr 161 of D2 [9,10]. The neutral tyrosine radicals, $Y_D^{\cdot}$ and $Y_Z^{\cdot}$ can be observed by EPR as Signal II. They can be distinguished kinetically or by their microwave power saturation characteristics which are influenced by interaction with the OEC [11–13].

Studies of ammonia binding to PS II have identified two sites of action. The first site, accessible to bulky amines as well as ammonia, is protected by Cl^-. It has been proposed that amines and ammonia displace the Cl^- from a site located on the Mn complex [14]. Binding at this Cl^--sensitive site results in an increased yield of the $g = 4.1$ EPR signal relative to the $g = 2$ multiline S_2 EPR signal [15–18] from the Mn complex. The second binding site is of lower affinity but is specific for ammonia and appears to result from bind-

Abbreviations: Chl, chlorophyll; EPR, electron paramagnetic resonance spectroscopy; EXAFS, extended X-ray absorption fine structure; Hepes, 4-(2-hydroxyethyl)-1-piperazineethanesulfonic acid; Hpp, peak to trough linewidth of EPR spectrum; MES, 2[*N*-morpholino]ethanesulfonic acid; OEC, oxygen-evolving complex; PPBQ, phenyl-1,4-benzoquinone; PS II, Photosystem II; S_1^*, S_2^* and S_3^*, modified S-states formed in treated samples analagous to native S_1, S_2 and S_3; XANES, X-ray absorption near edge structure; XAS, X-ray absorption spectroscopy.

* Corresponding author. Fax: +44 71 3807096.

SSDI 0005-2728(94)00141-3

ing in the S_2 state. Ammonia binding to this site is independent of Cl^- and results in the formation of a modified multiline S_2^* EPR signal [19]. From ESEEM results it was proposed that ammonia is incorporated into the Mn complex as a bridging ligand [20]. Further binding of ammonia in the S_3 state may be required for significant inhibition of oxygen evolution [1,3,17]. The concentrations of ammonia required to produce inhibition and those required to induce modification of EPR signals are different, with much greater concentrations required for inhibition of oxygen evolution in steady state measurements [1,15–17].

The results of ammonia-induced inhibition have analogies with samples depleted of either calcium or chloride. Alteration of the properties of the multiline signal are seen and following oxidation of S_2^* by illumination, each of the different inhibition treatments give rise to S_3 EPR signals with characteristic lineshapes [33–42]. The generation of an S_3 EPR signal following ammonia-induced inhibition suggests a block at the $S_3^* \rightarrow S_0$ transition [33,34] while distinct S_3 EPR lineshapes indicate different structural properties for the various treatments. Associated with the ammonia-induced inhibition is an increase in the amount of $Y_Z^{\cdot}$ detected at room temperature [13,33] due to disruption of electron transfer from the Mn complex.

Ammonia treatment can also affect the normal pattern of flash-induced oxygen evolution by delaying oxygen evolution by two to three flashes. The delay has been proposed to be due to the reduction of the Mn complex to give non-physiological S-states, S_{-1}, S_{-2} and perhaps S_{-3}, [1,21–30]. High concentrations of amine or long incubation times also cause irreversible damage and the loss of manganese as Mn^{2+} [23,31,32]. Reductant-induced inhibition is therefore thought to occur in two steps, reduction to Mn^{2+} followed by inhibitory release of Mn^{2+} from the complex [28].

In this study we report EPR and Mn K-edge XAS studies of ammonia and acetate-treated PS II. We have investigated the block at S_3^* and the role of the inorganic cofactors, chloride and calcium. We also investigated super-reduced intermediates, S_{-n}, that might be formed during ammonia reduction of PS II from the S_1^* state.

2. Materials and methods

Spinach PS II was prepared from market spinach according to the method of Berthold et al. [43] with the modifications of Ford and Evans [44] (Chl *a*/Chl *b* ratio 2.0–2.20 : 1). These are termed PS II membranes. Reagents used were all analytical grade. The MES, Hepes and sucrose solutions were treated with Chelex before use. NaCl-treated PS II (calcium-depleted) was prepared and reconstituted with the extrinsic polypeptides as given in Ref. [33] and calcium or sodium acetate-treated samples were prepared as in Ref. [42].

Ammonium acetate-treated or ammonium-treated PS II was prepared from PS II membranes by a simple procedure [42,45]. Membranes were first exchanged into the required pH buffer by centrifugation (40 000 × *g* for 30 min) and resuspension. 40 mM MES, was used for treatments up to pH 6.5 and 40 mM Hepes for treatment above pH 6.5. The membranes were then centrifuged at 40 000 × *g* for 30 min and resuspended in the final buffer containing the reagent concentrations and 0.3 M sucrose as given in the text. 0.5 mM or 1 mM PPBQ was added to samples that were to be illuminated. For samples where calcium was added, 20 mM calcium chloride was used.

The membranes obtained from the basic treatments were depleted of greater than 90% of their oxygen-evolving activity. This was measured in a Clark-type oxygen electrode at 298 K using ferricyanide and PPBQ as electron acceptors. The control was untreated membranes to which 20 mM calcium chloride was added and then incubated for 30 min on ice. Addition of calcium to ammonium-treated samples restores oxygen evolution to 60–70% of that found for untreated PS II membranes (control values were 350–600 μmol O_2/mg Chl per h) using identical illumination (see also Ref. [17]). Centrifugation of the 300 mM ammonium acetate-treated or ammonium-treated PS II preparation at 40 000 × *g* for 30 min, followed by SDS-polyacrylamide gel electrophoresis of the pelleted material showed that the 17 and 23 kDa extrinsic polypeptides but not the 33 kDa polypeptide are dissociated by the high salt concentrations (see Refs. [1–3] for reviews of the effects of high salt concentrations).

2.1. EPR spectrometry

For EPR at cryogenic temperatures, 0.3 ml samples (at approximately 10 mg Chl/ml) were placed in calibrated 3 mm internal diameter quartz EPR tubes. Samples at EXAFS concentration (> 50 mg Chl/ml) were also made using specially adapted holders. During dark adaptation, samples were kept on ice at 273 K. EPR spectrometry was performed using a Jeol RE1X spectrometer fitted with an Oxford Instruments liquid helium cryostat. Spectra were recorded and manipulated using a Dell microcomputer running Asyst software. For room temperature EPR, 10 μl or 15 μl samples in glass capillary tubes were placed inside EPR tubes. These samples were run as above using the cavity fitted to the Oxford Instruments cryostat except that 1 mM ferricyanide/1 mM ferrocyanide replaced PPBQ as electron acceptor [33].

To investigate the nature of the interaction between the radical and manganese cluster which gives rise to the S_3 EPR signal, a series of spectrum simulations

were performed. These perturbation calculations, including both dipolar and exchange interactions, utilised the protocol outlined by Eaton et al. [46], a methodology based on the equations derived by Smith and Pilbrow [47]. Simulations were performed with an IBM RS/6000 250 employing code (MENO [46]), which was modified locally to mimic a spin 1/2 system interacting with a spin 1/2 valence-trapped manganese dimer. Atomic coordinates for the interacting species were obtained from the PS II model of Ruffle et al. [48,49] and the pertinent distance and angular data were measured using SYBYL (Tripos). Y_Z was used as the free radical component of the interacting pair. Consistent with spectra analysis, the local magnetic Z axis (Z_1) was assigned orthogonal to the C–O bond for the hydroxy substituent [50]. For the tetranuclear manganese complex, the interacting component was assumed to be the putative di-μ-oxo bridged manganese structure closest to Tyr D1–161 (Y_Z). An average internuclear distance between the interacting spins of 0.92 nm was estimated from the model structure. The coordinate system assigned to the manganese dimer places the oxo-ligands in the xy plane, with the Z axis of each manganese colinear (Z_2) and orthogonal to this plane. The relative orientation of the di-μ-oxo complex coordinate system to that of Y_Z was assigned from the model structure: $\epsilon = 22°$, $\eta = 25°$, Ang 1 = 68°, Ang 2 = 5° and Ang 3 = 180°, adopting the convention of Eaton et al. [46]. The g-factors and A values for Y_Z were taken from Ref. [50]; the corresponding values for the manganese complex were obtained from a fit of the S_2 multiline EPR spectrum (J.T. Warden, in preparation); composite values used for the simulations were $g_x = 2.0083$, $g_y = 1.988$, $g_z = 1.92$; $A_{1x} = 559$ MHz, $A_{1y} = 478$ MHz, $A_{1z} = 472$ MHz and $A_{2x} = 250$ MHz, $A_{2y} = 248$ MHz, $A_{2z} = 245$ MHz.

2.2. Preparation of samples in different S-states

All procedures were carried out either in the dark or under a dim green light producing samples in the S_1^* state. S_1^* samples were then frozen in the dark. To obtain the S_3 signal, treated samples were illuminated on each side at 277 K for 30 s (total 1 min) using an unfiltered 650 W light source (1000 $\mu E/m^2/s$) and then the sample was frozen rapidly to 77 K under illumination. S_2^* was generated in treated samples by initially illuminating as for S_3, then storing the sample at 273 K for 5 min in the dark to allow relaxation to S_2^*, before freezing to 77 K. Illumination treatments for EPR and EXAFS samples were carried out immediately before measurement. Duplicate samples to those used for EXAFS were checked by EPR to ensure that illumination produced identical changes in modified S-state in both EPR and EXAFS samples. 200 K illumination was performed using an ethanol bath cooled with solid carbon dioxide.

2.3. EXAFS

Small amounts of Mn^{2+} are sometimes present in PS II preparations from damaged centres and as adventitiously absorbed manganese. This causes the measured edge energies of PS II samples to be lower and first shell bond distances to be longer than normal. The amount of Mn^{2+}, as indicated by the Mn^{2+} six line EPR spectrum and estimated by comparison to a 1 M HCl-treated sample, was $\ll 5\%$ unless otherwise stated.

EXAFS and EPR samples were made for each treatment from the same preparation. The EXAFS samples were centrifuged at 260 000 $\times g$ for 40 min and the pellet loaded into polycarbonate XAS sample holders or specially prepared EXAFS/EPR holders. Making the EPR samples from the remaining pellet immediately after the EXAFS samples ensured any sample deterioration was noted. Fluorescence XAS measurements were carried out using station 8.1 on the Synchrotron Radiation Source at the SERC Daresbury Laboratory. A slitless Si(220) double crystal monochromator was used and the fluorescent radiation detected by a thirteen element Ge solid-state detector as in Ref. [51]. Spectra were recorded at 77 K with a beam energy of 2 GeV and an average beam current of 160 mA. Five scans of approximately 1 h in duration were accumulated per sample. The data was analysed as in Refs. [51,52] using both the raw EXAFS and Fourier filtered EXAFS in k space with use of the Fourier transform confined to model building and visual determination of quality of fit. The EXAFS were weighted by k^3 and analyzed using the non-linear least-squares minimisation program EXCURV92, which calculates the theoretical EXAFS using the fast curved wave approach. Phase shifts were calculated by ab initio methods within the EXCURV90 program and verified with model compounds [52]. The photoelectron energy zero, E_0, was treated as a single overall parameter in the multiple-shell fits. E_0 refined to values close to those obtained for model compounds, 20–30 eV, below the experimental absorption threshold.

3. Results

3.1. EPR of ammonium acetate and ammonium chloride-treated samples

Illumination of untreated PS II samples in the S_1 state results in the appearance of the S_2 multiline EPR signal together with a $g = 1.9$ signal from the reduced

primary electron acceptor Q_A. A modified S_2^* state can be observed in ammonium chloride-treated samples at pH 7.5 as shown in Fig. 1a where samples were illuminated at 250 K and then frozen in the dark. This treatment allows a multiline spectrum with the characteristic modified pattern following ammonia treatment [15–17,19] to be seen. The S_2^* multiline is not affected by the presence of acetate at pH 7.5, signifying ammonia binding still occurs.

The S_3 EPR signal was originally discovered as the result of a one electron oxidation of a NaCl-treated/calcium-depleted sample showing a dark-stable multiline S_2^* state [37–41]. Illumination of an ammonium chloride-treated sample at 250 K or 277 K and then freezing under illumination to 77 K also causes the appearance of a signal split around $g = 2$ attributed to an S_3 signal, Fig. 1b [33,34]. The signal was easily detected in samples containing > 100 mM ammonium chloride as discussed previously [33,34]. A higher yield of the S_3 signal is obtained in the presence of an exogenous electron acceptor, 0.5 mM PPBQ [33,37,53].

We have previously discussed S_3 signals of three types. The signals in ammonium chloride-treated samples [33,34] have decreased splitting (Hpp), < 10 mT, compared to NaCl-treated samples, 13–16.5 mT [33,37–41], and acetate-treated samples, 22 mT [42]. The assignment of the signal to an organic radical magnetically interacting (exchange and/or dipolar coupled) with the Mn complex [37,39,41] suggests that these changes in splitting will perhaps involve slight structural differences between the interacting species. To investigate this further we have simulated each type of signal.

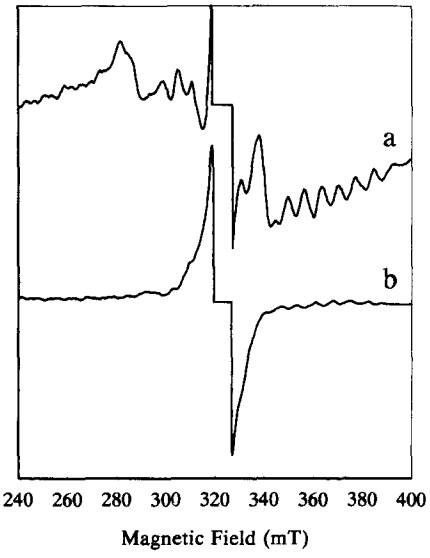

Fig. 1. EPR spectra of PS II membranes treated with 300 mM NH_4Cl, pH 7.5 showing S_2^* and S_3 signals. (a) Spectrum of sample following 5 min of 250 K illumination plus dark adaption for 5 min before cooling to 77 K, instrument gain 200. (b) Difference spectrum of sample illuminated for 5 min at 250 K then frozen to 77 K under illumination minus sample as in spectrum a, instrument gain 50. Spectrometer conditions: 10 mW microwave power, 2 mT modulation amplitude, temperature 9 K. The central region has been erased to remove the $Y_D^{\cdot}$ radical.

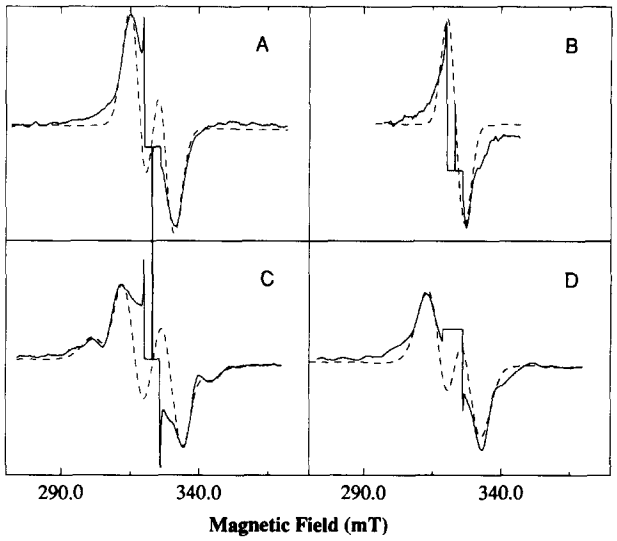

Fig. 2. Spectra (solid line) and simulations (dashed line) for variant forms of the S_3 signal. (A) NaCl-treated PS II membranes, calcium-depleted and reconstituted with the extrinsic polypeptides. (B) Ammonium chloride-treated PS II. (C) Sodium acetate-treated PS II. (D) Calcium acetate-treated PS II. EPR conditions were as in Fig. 1. Simulation parameters are given in Section 2.

Representative spectra for S_3 as observed for the three major lineshapes are presented in Fig. 2 accompanied by the pertinent simulations. The observed deviations between the experimental and computed spectra are attributed to our observation that in most cases the experimental spectra are an admixture of more than one lineshape form, e.g., sodium acetate-treated samples give a mixture of calcium-depleted and acetate-treated signals. In addition to this, the lineshape near $g = 2$ is masked by other radicals, mainly $Y_D^{\cdot}$, which have been removed. In general the simulated spectra were found to be insensitive to the relative angular orientation of the interaction species, but quite sensitive to the exchange interaction, J. Indeed, reasonable simulations can be obtained by varying only the exchange coupling parameter: $250 \cdot 10^{-4}$ cm^{-1} for sodium acetate-treated samples, $135 \cdot 10^{-4}$ cm^{-1} for calcium acetate-treated samples, $105 \cdot 10^{-4}$ cm^{-1} for NaCl-treated samples and $25 \cdot 10^{-4}$ cm^{-1} for ammonium chloride-treated PS II (Fig. 2). This observation appears consistent with the presumed interspin distance of 0.9 nm; presumably anisotropic exchange would be negligible in this case. The simulations indicate that the S_3 signal in its various forms can be regarded as a token of the strength of exchange coupling between the organic radical and the manganese cluster. Fig. 2 shows that ammonium chloride treat-

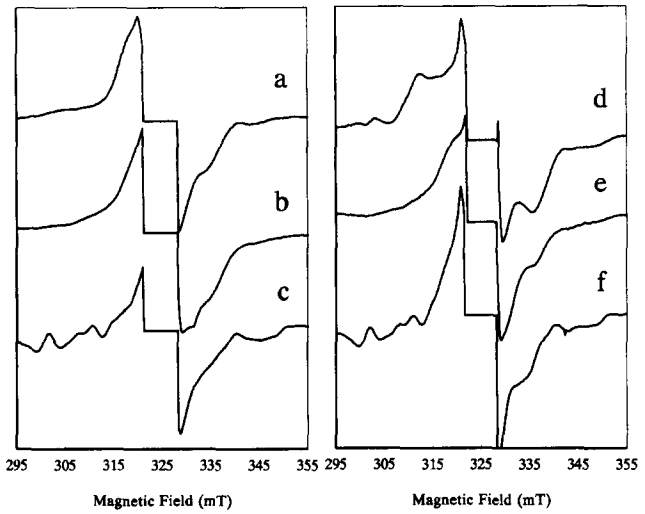

Fig. 3. Spectra showing the S_3 EPR signal in 300 mM NH_4Cl-treated samples at different pH values, (a) pH 5.5, (b) pH 6.5 and (c) pH 7.5. 300 mM ammonium acetate-treated samples are shown in (d) pH 5.5, (e) pH 6.5 and (f) pH 7.5. Spectra shown are the difference between samples illuminated at 277 K for 1 min and then frozen to 77 K under illumination and the same sample with identical illumination but then frozen to 77 K after 30 min in the dark. Spectrometer conditions as in Fig. 1.

ment results in the narrowest signal for S_3 and hence the smallest value for J, with the largest values of J and linewidth found for acetate-treated samples. The relative insensitivity of the simulated spectra on distance ($r > 0.6$ nm) and species orientation would suggest that for this model, structural rearrangement in PS II is significant only in that exchange pathways can be enhanced in the ion-treated samples.

Although currently the identity of the interacting species is uncertain, these simulations do not exclude the participation of histidine in the interaction [39]. Assuming the manganese complex to be close to the position proposed in the model of Ruffle et al., then only three histidine residues (D1 337, 332 and 190) are close by. For example, D1 His-190 might be expected to yield a qualitatively similar interaction as Tyr D1–161, based on their similar position in the proposed structure.

3.2. pH dependence of S_3 EPR signals

Studies on sodium acetate-treated PS II indicated that acetate competed with chloride and revealed a pH dependence in the yield of S_3 signal, perhaps signifying an event associated with an amino acid protonation [42]. Incubations of ammonium chloride-treated PS II at various pH values revealed that the linewidth of the S_3 signal was sensitive to pH, Fig. 3a–c. Comparison of the spectra with the three types of S_3 signals discussed above shows that the EPR signals represent the sum of two or more EPR lineshapes. At pH 5.5 the signal has components having a narrow < 10.0 mT splitting and a wider 15.0 mT splitting, similar to that observed in NaCl-treated PS II [33,37–41]. At higher pH values the linewidth of the signal was decreased and at pH 7.5 with high ammonium concentrations (e.g. 300 mM as shown) a release of Mn^{2+} which increased with time of incubation was observed.

Fig. 3d–f shows the pH dependence of the S_3 signals in ammonium acetate-treated samples. A maximum yield for the 22 mT split sodium or calcium acetate-induced signal was achieved at pH 5.5 [42]. A similar splitting is observed in ammonium acetate-treated PS II at acidic pH. Although at acidic pH an approximately 22 mT signal is apparent, there is also a shoulder from a signal with narrower splitting. As the pH is raised, the splitting of the signal decreases to a value similar to that of the ammonium chloride-induced signal by pH 7.0. Again Mn^{2+} release is detected at pH 7.5.

3.3. The effect of added calcium on ammonia-treated samples

In native PS II, the Mn complex is oxidised by Y_Z. Normally, this is not detected by conventional EPR as the lifetime of this radical is too short. However, in inhibited PS II or PS II depleted of Mn, the lifetime of $Y_Z^{\cdot}$ is increased. Detection of this $Y_Z^{\cdot}$ by EPR is as the light-induced increase in tyrosine radical near $g = 2$ at room temperature, as $Y_D^{\cdot}$ is relatively dark stable. Treatment of PS II membranes with 300 mM ammo-

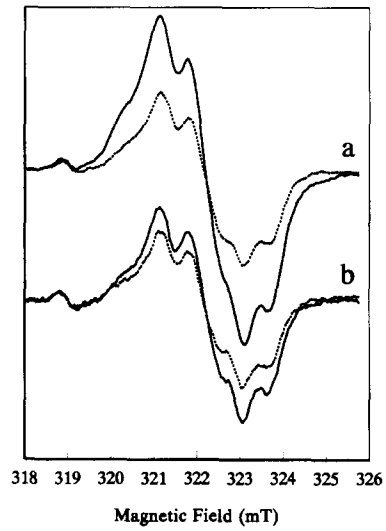

Fig. 4. Room temperature EPR spectra of $Y_D^{\cdot}$ and $Y_Z^{\cdot}$. (a) PS II with 300 mM NH_4Cl added at pH 7.5; (b) as (a) but with 20 mM $CaCl_2$ added following NH_4Cl addition. Solid line, signal under continuous illumination. Broken line, sample recorded 2 min after illumination. Spectrometer conditions: microwave power 10 mW, temperature 294 K, modulation amplitude 0.32 mT. Other conditions as given in Section 2.

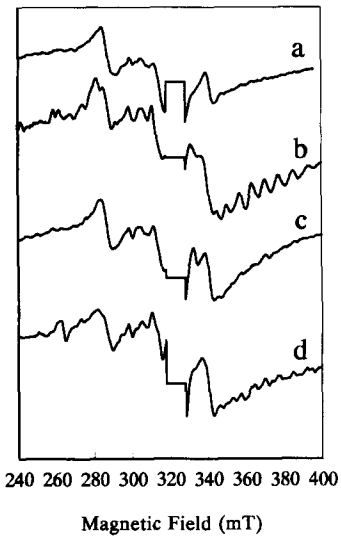

Fig. 5. EPR spectra of samples containing a 20 mM calcium chloride addition to 300 mM NH_4Cl-treated PS II at pH 7.5. (a) 10 min dark-adapted sample; (b) sample as (a) illuminated at 250 K for 5 min and frozen to 77 K in the dark showing the S_2^* signal; (c) sample as (a) illuminated at 77 K for 10 min; (d) sample illuminated at 277 K for 1 min and frozen to 77 K with illumination. Note the absence of S_3 signal. Spectrometer conditions as in Fig. 1.

nium chloride, pH 7.5, results in the formation of $Y_Z^{\cdot}$ during room temperature illumination, Fig. 4a. This agrees with previous studies [13,33], and indicates that the step inhibited in these systems is between $Y_Z^{\cdot}$ and the OEC. However, when calcium chloride was added to the treated sample, the yield of $Y_Z^{\cdot}$ was decreased, Fig. 4b, showing the restoration of fast kinetics and S-state cycling.

A second effect of calcium chloride addition to ammonium chloride-treated PS II was to inhibit formation of the S_3 signal, Fig. 5. In the case of ammonium acetate inhibition, calcium addition results in a removal of the < 16 mT components of the S_3 signal and a decrease in the extent of oxygen evolution inhibition [42]. A 22 mT S_3 signal due to the effect of acetate alone is still obtained at acidic pH (not shown but demonstrated previously [42]). The ammonia modified multiline is still generated by illumination following calcium addition, Fig. 5b.

Oxygen evolution measurements on ammonium chloride-treated PS II indicated $> 90\%$ inhibition had been achieved. Incubation of the ammonia-treated PS II with 20 mM calcium chloride restored 60–70% of the oxygen evolving capacity of an untreated sample. This agrees with the observations [16,17] of only limited inhibition of steady-state oxygen evolution by ammonia treatment alone. The inhibition of steady-state oxygen evolution by a block at S_3^* is therefore attributed to effects of high cation concentration on the calcium cofactor and not to ammonia binding.

3.4. Ammonia release of divalent manganese

Samples treated with ammonium chloride at pH 7.0 and 7.5, without calcium chloride in the buffer, contained increasing amounts of Mn^{2+} as the length of dark incubation and cation concentration increased. This was measured using the Mn^{2+} six line EPR spectrum noted above. An estimate of the percentage of Mn present as Mn^{2+} after 3 h at 277 K was made by comparison to a 2 M HCl-treated sample which is assumed to have all the Mn present as Mn^{2+}. Increased levels of Mn^{2+} are observed at pH 7.5 for the same incubation time and concentration compared to pH 7.0 treatment (compare Figs. 6a and 7a for 300 mM treatment). For the samples shown in Figs. 6 and 7, the fraction of Mn^{2+} in the samples was $< 25\%$ at pH 7.0 (Fig. 6) and $> 75\%$ at pH 7.5 (Fig. 7). When the dark-adapted ammonia-treated samples were thawed and illuminated for 1 min at 277 K then frozen to 77 K with illumination, a signal with lineshape of an S_3 signal formed with concomitent loss of the Mn^{2+} EPR signal, Fig. 6b. This would suggest that the Mn^{2+} is still associated with or close by to the Mn binding sites of the OEC. The size of S_3 signal was lower at pH 7.5 (Fig. 7b).

To test whether the Mn^{2+} was stably oxidised we thawed and dark adapted the illuminated sample for 5 min. The resulting samples show Mn^{2+}, the signal intensity of which is close to that before illumination, Figs. 6c and 7c. If a treated sample containing Mn^{2+} is

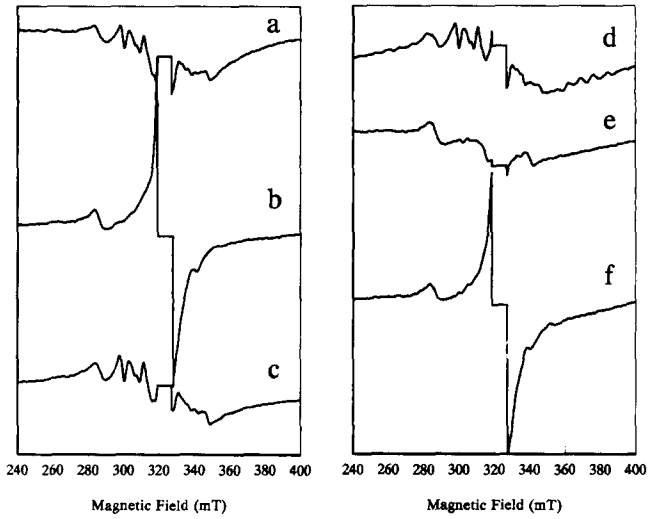

Fig. 6. EPR spectra showing the photoreversible release of Mn^{2+} in 300 mM NH_4Cl-treated PS II, pH 7.0. (a) Dark-adapted for 3 h; (b) sample as (a) then illuminated at 277 K and frozen under illumination to 77 K to form S_3^*; (c) as (b) then thawed and dark-adapted for 5 min; (d) as (c) then illuminated at 200 K for 10 min; (e) as (c) then thawed and 10 mM EGTA added and sample dark-adapted for 5 min;: (f) as (e) then illuminated at 277 K and frozen under illumination to 77 K to form S_3^*. Spectrometer conditions as Fig. 1.

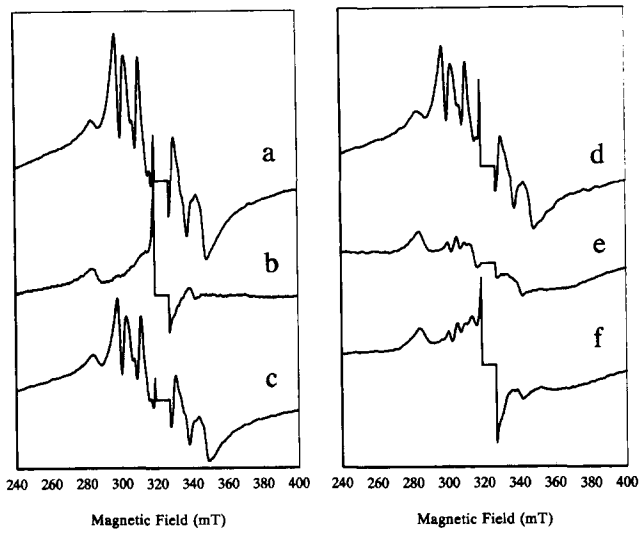

Fig. 7. EPR spectra showing the photoreversible release of Mn^{2+} in 300 mM NH_4Cl-treated PS II, pH 7.5 (a) Dark-adapted for 3 h; (b) sample as (a) then illuminated at 277 K and frozen under illumination to 77 K to form S_3^*; (c) as (b) then thawed and dark-adapted for 5 min; (d) as (c) then illuminated at 200 K for 10 min; (e) as (c) then thawed and 10 mM EGTA added and sample dark-adapted for 5 min; (f) as (e) then illuminated at 277 K and frozen under illumination to 77 K to form S_3^*. Spectrometer conditions as in Fig. 1.

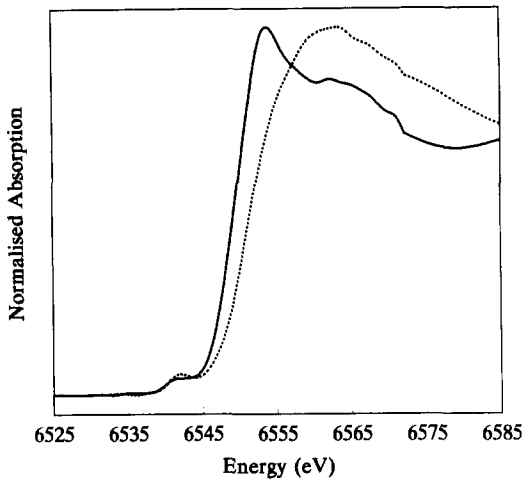

Fig. 8. The Mn K-edge XANES region for 300 mM NH_4Cl-treated PS II, pH 7.5 showing edge shift following illumination. Sample treated as in Fig. 7. Solid line, dark-adapted for 3 h; dotted line, sample illuminated at 277 K and then frozen under illumination. The spectra were smoothed with a ninth order polynomial smoothing function. Other conditions as given in Fig. 7 and Section 2.

illuminated at 200 K, the Mn^{2+} is not oxidised (Figs. 6d and 7d), though a weak multiline signal from the ammonia-modified S_2^* state appears in the pH 7.0 sample, Fig. 6d.

To determine whether the Mn^{2+} is accessible, we have added 10 mM EGTA to samples previously illuminated at 277 K and then thawed as in Figs. 6a–c, 7a–c. On addition of EGTA in the dark, the Mn^{2+} six line EPR signal is abolished, Figs. 6e, 7e. Illumination of the EGTA-treated samples still allows formation of some S_3 signal. The yield of the S_3 type signal is similar to that before EGTA addition for the pH 7.0 samples but decreased for the pH 7.5 samples. It therefore appears that release of Mn^{2+} correlates with loss of the S_3 signal, at least part of the Mn^{2+} can be reincorporated into the Mn complex by illumination and that the Mn^{2+} released is accessible to removal by EGTA. As we do not know the location of the Mn^{2+}, we do not know if the EGTA-accessible Mn^{2+} represents centres unable to form the S_3^* state even after 277 K illumination. The 17 and 23 kDa extrinsic polypeptides are dissociated, probably allowing easier access of EGTA to the manganese.

3.5. X-ray absorption studies

The Mn K-edge data presented in Fig. 8 are from the 3 h dark-adapted and 277 K illuminated ammonium chloride-treated samples at pH 7.5 as shown in Fig. 7a and b. The steeply rising edge, sharp peak and edge position of the dark-adapted sample indicate Mn^{2+} as observed by EPR. The pre-edge of the 300 mM ammonium chloride sample at pH 7.5 in the dark shows a small intensity 1s-3d feature, smaller than found in native PS II or reported in ammonia-treated PS II [54,55], not containing Mn^{2+}. Changes in the XANES region are best observed by taking second derivatives of the edge region to enhance any features present, Fig. 9. The feature at about 6552 eV in the reduced sample seems indicative of Mn^{2+} and might

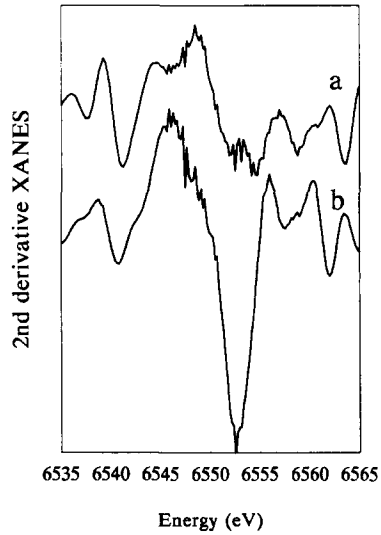

Fig. 9. Second derivative of the Mn K-edge XANES region for 300 mM NH_4Cl-treated PS II, pH 7.5 as in Fig. 8. (a) Dark-adapted for 3 h then illuminated at 277 K and frozen under illumination; (b) dark-adapted for 3 h. The spectra were smoothed with a ninth order polynomial smoothing function before differentiation. Other conditions as given in Fig. 7 and Section 2.

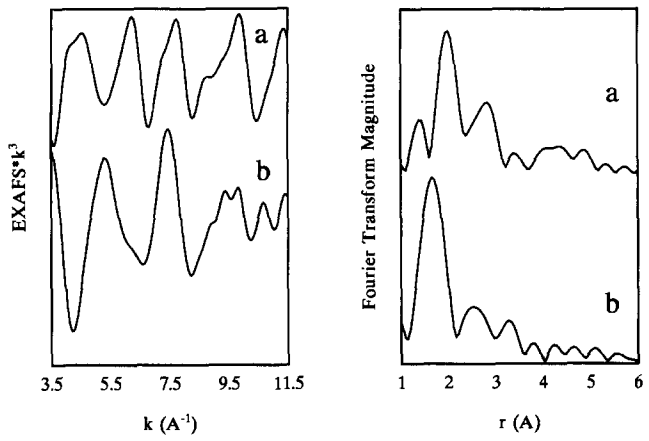

Fig. 10. Fourier-filtered k^3-weighted EXAFS data and k^3-weighted Fourier transforms of PS II samples treated with 300 mM NH_4Cl, pH 7.5 as in Fig. 7. (a) Dark-adapted for 3 h; (b) as (a) then illuminated at 277 K and frozen under illumination. The Fourier window was 0.7–4.5 Å, uncorrected for phase.

be of use in assessing native sample integrity. On illumination the shape of the edge and the intensity of the pre-edge feature resembles that of previous ammonia-treated samples [54,55] and is accompanied by an increase in edge energy on illumination at 277 K which indicates that Mn oxidation occurs.

EXAFS data and their Fourier transforms for the 300 mM ammonium chloride samples shown in Fig. 7–9 are given in Fig. 10. These show changes on illumination consistent with the EPR and Mn K-edge measurements. We were unable to obtain satisfactory fits to the data sets of dark-adapted samples. This is most likely due to the complex nature of the spectra. It has been observed that for reduced binuclear Mn and Fe sites in proteins, an unambiguous definition of the metal-metal distance is not always possible. This has been attributed to the loss of bridging ligands [56–58]. At present we cannot determine whether the manganese are closely associated or not. However, we can obtain useful information on the first shell of scatterers. In the dark, the first shell of scatterers are located at 2.1–2.2 Å, Fig. 10a. The first shell bond distance is longer than in the native state, where distances of 1.84–1.86 Å are obtained (e.g. [52,59]). The shorter distances are usually associated with Mn(III)/Mn(IV) μ-oxo bridging ligands.

The increased bond lengths in treated samples are consistent with a large Mn^{2+} content for which first shell bond lengths of about 2.1 Å are expected. In untreated PS II membrane fragments, there is a Mn–Mn interaction at 2.7 Å. The second shell of scatterers in treated samples is either not observed in the reduced samples or shifted to features at > 2.7 Å. We are unable to fit this shell of scatterers to Mn, Cl or low Z scatterers such as C, O or N. Clearly the structure of the Mn complex is severely disrupted in the dark-adapted sample, though the presence of Fourier features at > 2.5 Å suggests Mn–Mn interactions may be present. Illumination at 277 K returns the EXAFS to a more usual trace with features at < 2 Å and 2.7 Å. The best fit of the data from the illuminated sample (Fig. 10b) is similar to that obtained for ammonia-treated samples in the S_3^* state. This fit indicates 4–5 (O or N) at 1.85Å, 1 (Mn) at 2.73Å and 1 (Ca, Mn, C or O) at 3.7Å.

If the manganese were nonspecifically bound, then we would not expect the observed redox chemistry to occur. We propose that in dark-adapted samples the reduced manganese is retained at or near the site for the Mn complex in PS II.

4. Discussion

As discussed above, ammonia binds to at least two sites in the OEC, one in competition with and one independent of chloride binding [13–20]. We are now able to explain some of the contradictory findings in the literature (see Ref. [17] for discussion) with regard to the effects of this treatment.

The addition of ammonia is complicated by the requirement of a high concentration of ammonium cations in order to generate significant quantities of ammonia in the pH ranges needed to study PS II. In these cases the ammonium cation acts, in a similar way to sodium and other cations, to displace calcium and causes inhibition of oxygen evolution, blocking the $S_3^* \rightarrow S_0$ transition. Inhibition observed in steady-state studies is therefore a consequence of the high cation concentration and not an effect due to ammonia binding alone. The ammonium cation is of similar size to Ca^{2+} and could bind at the calcium site if calcium depletion is the result of competitive binding. Ca^{2+} binding to PS II is, however, difficult to quantitate. Alternatively ammonia may bind nearby, causing a structural change at the calcium site. The block of the $S_3^* \rightarrow S_0$ transition allows the accumulation of an S_3 EPR signal on freezing to 77 K with illumination, and the observation of $Y_Z^{\cdot}$ in room temperature EPR studies.

The ability to generate the S_3 signal in ammonium chloride/acetate-treated samples is sensitive to pH, with changes in the signal intensity and linewidth, especially on decreasing pH. As calcium addition abolishes the < 10 mT pH > 7 and the 13.0–15.0 mT pH < 7 S_3 signals, these signals are due to a calcium effect, probably calcium depletion. The concentration of ammonia in solution is very pH dependent, $pK_a(NH_4^+/NH_3) = 9.24$ so that at pH < 7 only very small amounts of free base are present. The dominant effect in ammonium chloride-treated samples at acidic pH is from the ammonium cation, giving a 13.0–15.0

mT S_3 signal, i.e., similar to calcium-depleted samples prepared using sodium chloride. As the pH is raised the ammonia concentration increases and ammonia binding accompanied by chloride depletion or a deprotonation modifies the electron spin interaction. This gives a smaller splitting than found in samples calcium depleted by sodium halide salts or ammonium chloride at lower pH [33,37–42]. It is interesting that the EPR effects of ammonium and strontium treatment are so similar, giving a similar linewidth for both S_2^* multiline and S_3 signals [42]. The linewidths of the S_3 signals are, however, also similar to those found after chloride depletion. Perhaps ammonium or strontium treatment both result in replacement of calcium but also loss of or change in chloride binding.

For acetate, if the free acid is the active species [42], the pH also determines the amount of active species present. At high pH in the presence of ammonia, the < 10 mT linewidth dominates as the ammonia concentration is significant and there is little free acid. When the concentration of free acetic acid increases as the pH is lowered, so the splitting of the S_3 signal increases and the lineshape becomes a mixture of the 13.0–15.0 mT form and the broader acetate form.

In agreement with earlier observations on inhibition treatments at high pH [33], we also observe the formation of Mn^{2+} in samples prepared at pH 7.0 and 7.5; the concentration of which increases with time. Instability at pH > 7 appears to be through changes to the Mn complex, as Y_Z could still be oxidized at pH 7.5. As Ca^{2+} protects against Mn^{2+} formation, the instability results from the effects of cofactor depletion. It is possible that calcium depletion results in an increased susceptibility to hydroxide at the chloride site. Mei and Yocum [27,28] also showed that calcium had a protective effect against hydroquinone or hydroxylamine-induced loss of activity, slowing release of Mn^{2+}, and that the EPR detected appearance of Mn^{2+} after hydroquinone treatment was photoreversible. The hydroquinone-induced Mn^{2+} was, however, not EDTA-accessible unlike Mn^{2+} release by hydroxylamine, leading to a suggestion [29] that hydroxylamine may attack a water-accessible site. The investigation by EXAFS of the production of reduced derivatives of the Mn complex by hydroxylamine has produced two views, a reduction to S_0 but only following illumination [30] or a reduction in the dark [29]. Here we show that with ammonia, a reduction occurs in the dark during incubation for long periods.

A mechanism for amine-induced inactivation of PS II has been proposed by Rickert et al. [32] in which amines displace chloride and promote release of Mn^{2+}. Studies have also concluded that for amines a rapid four-electron reduction of the Mn complex occurs. This results in super-reduced states, S_{-2} from S_2 and S_{-3} from S_1, which contain the lower oxidation states for Mn. Such states would be expected to be labile and rapidly decompose into free Mn^{2+}. We propose from our EPR and EXAFS data that ammonia acts in an analogous fashion to the other reductants and also forms super-reduced S-states. The role of calcium must be added to the mechanism. Calcium appears to both stabilise the Mn cluster to disproportionation (Mn^{2+} formation) by maintaining the protein conformation, as well as to modify the redox potential of the Mn cluster as indicated by the alteration in S-state stability on depletion. As ammonia is able to bind in the presence of calcium, we favour a conformational and redox modifying role for calcium rather than any 'gate-keeper' role whereby calcium controls substrate accessibilty. In support of this role is the recent observation [60] that calcium incorporated into oxo-bridged manganese dimer compounds has a profound effect on the electrochemical properties of these mimics. Of course a structural role in which calcium controls protein folding could be thought of as equivalent to redox control. While strontium can replace calcium the efficiency of water oxidation is reduced, perhaps also reinforcing a structural role for calcium.

Acknowledgements

We acknowledge financial assistance from the U.K. Science and Engineering Research Council. We wish to acknowledge the generosity of Prof. Sandra Eaton for supplying the source code for the MENO program. J.T.W. was supported in part by the National Institutes of Health (GM 26133).

References

[1] Debus, R.J. (1992) Biochim. Biophys. Acta 1102, 269–352.
[2] Renger, G. (1992) in The Photosystems: Structure, Function and Molecular Biology, (Barber, J., ed.), Chapter 3, pp. 45–99, Elsevier, Amsterdam.
[3] Rutherford, A.W., Zimmermann, J.-L. and Boussac, A. (1992) in The Photosystems: Structure, Function and Molecular Biology, (Barber, J. ed.), Chapter 5, pp. 179–229, Elsevier, Amsterdam.
[4] Evans, M.C.W. and Nugent, J.H.A. (1993) in The Photosynthetic Reaction Center Vol. I (Deisenhofer, J. and Norris, J.R., eds.), Chapter 13, pp.391–415, Academic Press, San Diego.
[5] Debus, R.J., Barry, B.A., Sithole, I., Babcock, G.T. and McIntosh, L. (1988) Biochemistry 27, 9071–9074.
[6] Metz, J.G., Nixon, P.J., Rogner, M., Brudvig, G.W. and Diner, B.A. (1989) Biochemistry 28, 6960–6969.
[7] Coleman, W.J. (1990) Photosynth. Res. 23, 1–27.
[8] Yocum, C.F. (1991) Biochim. Biophys. Acta 1059, 1–15.
[9] Debus, R.J., Barry, B.A., Babcock, G.T. and McIntosh, L. (1988) Proc. Natl. Acad. Sci. USA 85, 427–430.
[10] Vermaas, W.F.J., Rutherford, A.W. and Hansson, O. (1988) Proc. Natl. Acad. Sci. USA 85, 8477–8481.

[11] Babcock, G.T., Barry, B.A., Debus, R.J., Hoganson, C.W., Atamian, M., McIntosh, L., Sithole, I. and Yocum, C.F. (1988) Biochemistry 28, 9557–9565.
[12] Warden, J.T., Blankenship, R.E. and Sauer, K. (1976) Biochim. Biophys. Acta 423, 462–478.
[13] Yocum, C.F. and Babcock, G.T. (1981) FEBS Lett. 130, 99–102.
[14] Sandusky, P.O. and Yocum, C.F. (1986) Biochim. Biophys. Acta 849, 85–93.
[15] Beck, W.F. and Brudvig, G.W. (1986) Biochemistry 25, 6479–6486.
[16] Andreasson, L.-E., Hansson, O. and Von Schenck, K. (1988) Biochim. Biophys. Acta 936, 351–360.
[17] Boussac, A., Rutherford, A.W. and Styring, S. (1990) Biochemistry 29, 24–32.
[18] Kim, D.H., Britt, R.D., Klein, M.P. and Sauer, K. (1992) Biochemistry 31, 541–547.
[19] Beck, W.F., dePaula, J.C. and Brudvig, G.W. (1986) J. Am. Chem. Soc. 108, 4018–4022.
[20] Britt, R.D., Zimmermann, J.L., Sauer, K. and Klein, M.P. (1989) J. Am. Chem. Soc. 111, 3522–3532.
[21] Bouges, B. (1971) Biochim. Biophys. Acta 234, 103–112.
[22] Beck, W.F. and Brudvig, G.W. (1987) Biochemistry 26, 8285–8295.
[23] Beck, W.F. and Brudvig, G.W. (1988) J. Am. Chem. Soc. 110, 1517–1523.
[24] Messinger, J., Wacker, U. and Renger, G. (1991) Biochemistry 30, 7852–7862.
[25] Messinger, J. and Renger, G. (1993) Biochemistry 32, 9379–9386.
[26] Kretschmann, H. and Witt, H.T. (1993) Biochim. Biophys. Acta 1144, 331–345.
[27] Mei, R. and Yocum, C.F. (1991) Biochemistry 30, 7836–7842.
[28] Mei, R. and Yocum, C.F. (1992) Biochemistry 31, 8449–8454.
[29] Riggs, P.J., Mei, R., Yocum, C.F. and Penner-Hahn, J.E. (1992) J. Am. Chem. Soc. 114, 10650–10651.
[30] Guiles, R.D., Yachandra, V.K., McDermott, A.E., Cole, J.L., Dexheimer, S.L., Britt, R.D., Sauer, K. and Klein, M.P. (1990) Biochemistry 29, 486–496.
[31] Tamura, N. and Cheniae, G.M. (1985) Biochim. Biophys. Acta 809, 245–259.
[32] Rickert, K.W., Sears, J., Beck, W.F. and Brudvig, G.W. (1991) Biochemistry 30, 7888–7894.
[33] Hallahan, B.J., Nugent, J.H.A., Warden, J.T. and Evans, M.C.W. (1992) Biochemistry 31, 4562–4573.
[34] Andreasson, L.-E. and Lindberg, K. (1992) Biochim. Biophys. Acta 1100, 177–183.
[35] Baumgarten, M., Philo, J.S. and Dismukes, G.C. (1990) Biochemistry 29, 10814–10822.
[36] Boussac, A. and Rutherford, A.W. (1992) Biochemistry 31, 7441–7445.
[37] Boussac, A., Zimmermann, J.-L. and Rutherford, A.W. (1989) Biochemistry 28, 8984–8989.
[38] Boussac, A., Zimmermann, J.-L. and Rutherford, A.W. (1990) FEBS Lett. 277, 69–74.
[39] Boussac, A., Zimmermann, J.-L., Rutherford, A.W. and Lavergne, J. (1990) Nature 347, 303–306.
[40] Ono, T. and Inoue, Y. (1990) Biochim. Biophys. Acta 1020, 269–277.
[41] Sivaraja, M., Tso, J. and Dismukes, G.C. (1989) Biochemistry 28, 9459–9464.
[42] MacLachlan D.J. and Nugent J.H.A. (1993) Biochemistry 32, 9772–9780.
[43] Berthold, D.A., Babcock, G.T. and Yocum, C.F. (1981) FEBS Lett. 134, 231–234.
[44] Ford, R.C. and Evans, M.C.W. (1983) FEBS Lett. 160, 159–163.
[45] Saygin, O., Gerken, S., Meyer, B. and Witt, H.T. (1986) Photosynth. Res. 9, 71–78.
[46] Eaton, S.S., More, K.M., Savant, B.M., Boymel, P.M. and Eaton, G.R. (1983) J. Magn. Reson. 52, 435–449.
[47] Smith, T.D. and Pilbrow, J.R. (1974) Coord. Chem. Rev. 13, 173–278.
[48] Ruffle, S.V., Donnelly, D., Blundell, T.L. and Nugent, J.H.A. (1992) Photosynth. Res. 34, 287–300.
[49] Ruffle, S.V. and Nugent, J.H.A. (1992) in Research in Photosynthesis, Vol. II (Murata, N., ed.), pp. 191–194, Kluwer, Dordrecht, The Netherlands.
[50] Hoganson, C.W. and Babcock, G.T. (1992) Biochemistry 31, 11874–11880.
[51] MacLachlan, D.J., Nugent, J.H.A., Bratt, P.J. and Evans, M.C.W. (1994) Biochim. Biophys. Acta 1186, 186–200.
[52] MacLachlan, D.J., Hallahan, B.J., Ruffle, S.V., Nugent, J.H.A., Evans, M.C.W., Strange, R.W. and Hasnain, S.S. (1992) Biochem. J. 285, 569–576.
[53] Tso, J., Sivaraja, M., Philo, J.S. and Dismukes, G.C. (1991) Biochemistry 30, 4740–4747.
[54] Nugent, J.H.A., MacLachlan, D.J., Rigby, S.E.J. and Evans M.C.W. (1993) Photosynth. Res. 38, 341–346.
[55] MacLachlan, D.J., Nugent, J.H.A. and Evans, M.C.W. (1994) Biochim. Biophys. Acta 1185, 103–111.
[56] Kauzlarich, S.M., Teo, B.K., Zirino, T, Barman, S., Davis, J.C. and Averill, B.A. (1986) Inorg. Chem. 25, 2781–2785.
[57] DeWitt, J.G., Bentsen, J.G., Rosenzweig, A.C., Hedman, B., Green, J., Pilkington, S., Papaefthymiou, G.C., Dalton, H., Hodgson, K.O. and Lippard, S.J. (1991) J. Am. Chem. Soc. 113, 9219–9235.
[58] Waldo, G.S., Yu, S. and Penner-Hahn, J.E. (1992) J. Am. Chem. Soc. 114, 5869–5870.
[59] Yachandra, V.K., DeRose, V.J., Latimer, M.J., Mukerji, I., Sauer, K. and Klein, M. (1993) Science 260, 675–679.
[60] Horwitz, C.P. and Ciringh, Y. (1994) Inorg. Chem. Acta, in press.